AN EXPERIMENTAL INVESTIGATION OF THE ANGULAR SCATTERING AND BACKSCATTERING BEHAVIORS OF THE SIMULATED CLOUDS OF THE OUTER PLANETS

FINAL REPORT

- Prepared For -

National Aeronautics and Space Administration

Grant No. NAGW-82

(1 June 1980 - 30 September 1984)

- Prepared By -

Kenneth Sassen

Department of Meteorology
University of Utah
Salt Lake City, Utah 84112

TABLE OF CONTENTS

ABSTRACT

A cryogenic, 50 liter volume Planetary Cloud Simulation Chamber has been constructed to permit the laboratory study of the cloud compositions which are likely to be found in the atmospheres of the outer planets. On the basis of available data, clouds composed of water ice, carbon dioxide, and liquid and solid ammonia and methane, both pure and in various mixtures, have been generated. Cloud microphysical observations have been permitted through the use of a cloud particle slide injector and photomicrography. Viewports in the lower chamber have enabled the collection of cloud backscattering data using 633 and 838 nm laser light, including linear depolarization ratios δ and complete Stokes parameterization. The considerable technological difficulties associated with the collection of angular scattering patterns within the chamber, however, could not be completely overcome.

The backscatter linear depolarization technique has been shown to display considerable potential as a planetary probe for identifying the ice phase particles produced in this study. Within the overall temperature range of ~80-200°K, pure solid CO_2, NH_3 and CH_4 clouds yielded average δ values of 0.07, 0.42 and 0.94, respectively. Water ice clouds yielded δ values of 0.5 for hexagonal crystals (>215°K), ratios of a few percent for spherical vitreous particles (between 85-175°K), and gradually increasing δ values with increasing temperatures in the intermediate range due to mixtures of the vitreous, hexagonal, and probably cubic growth modes.

From the cloud microphysical studies it has been possible to infer a number of interesting features of the cloud formation processes on the outer planets. Importantly, it should be recognized that all liquid clouds displayed

the ability to remain in a considerably supercooled state in the aerosol-free environment of the chamber. Liquid ammonia, for example, could be supercooled to at least ~50°K below the melting point before homogeneous ice nucleation occurred. Hence, the phase of extraterrestrial clouds will depend not only on their temperatures but also to a considerable extent on the existence of suitable ice-initiating nuclei at the cloud level. In the Martian atmosphere, CO_2 cloud formation requires the presence of suitable deposition nuclei or water ice germs, and under appropriate conditions combined H_2O/CO_2 ice particle growth has been observed to occur. Water vapor also readily combines with ammonia in the liquid and probably solid phase, and there is strong evidence that the evaporation of water-ammonia solution droplets will result in the formation of ammonium salt aerosol hazes in subsaturated atmospheric regions.

1. Introduction

Although the compositions of the clouds of the outer planets have yet to be directly sampled, our knowledge of the gaseous constituents and approximate temperatures of their atmospheres allows us to infer the likely cloud compositions. Considerable data on the planetary scattering properties of their atmospheres are also available from recent space probes, information which has potential for identifying the constituents of the outer cloud layers of the planets. For example, polarimeter measurements of the polarization state of the sunlight scattered by planetary cloud cover as functions of the scattering angle and wavelength have been used to determine the composition of the clouds of Venus (see, e.g., Hansen and Hovenier, 1974). Unfortunately, the much colder and more exotic outer atmospheres of the outer planets will certainly contain solid phase clouds of nonspherical particles of unknown shape, presenting considerable barriers to this kind of planetary scattering data analysis. Although the recent advances in hexagonal ice crystal scattering theory via the ray tracing method are significant (e.g., Cai and Liou, 1982), the shapes and optical properties of the ice clouds of the outer planets must first be known before applying this method. Assuming the presence of cubic crystals, for example, Whalley and McLaurin (1984) have attempted to model the halos which may be present elsewhere in the solar system.

In addition to such passive remote sensing techniques, there is another technology which should find increasing application for extraterrestrial atmospheric studies. That is, "droppable" instrument packages can be released from orbiting or fly-by platforms for *in situ* cloud measurements during fall through the atmosphere. The use of active light scattering techniques employing

laser sources will undoubtedly contribute prominently to the *in situ* cloud studies permitted by this developing technology once the optimum design of such a device is evaluated. The demonstrated utility of the optical backscatter depolarization technique for terrestrial cloud phase discrimination would suggest that laser light backscattering measurements would provide optimal information content. In general, it has been shown (see Sassen and Liou, 1979) that backscattering depolarization observations combine the maximum sensitivity to cloud particle shape with relatively strong signal returns. Investigations of extraterrestrial cloud backscattering behavior also have the advantage of delineating the potential of lidar cloud studies from orbiting platforms. Although advances in lidar technology are clearly required for such applications, the added advantage of the ranging capability of lidar for measuring the vertical distribution and content of individual cloud layers makes the possibility of lidar application quite attractive.

As with the terrestrial cloud studies (see Sassen, 1978), the laser depolarization ratios measured in the backscatter can be used to discriminate between cloud particle species only after "signatures" characteristic of each species are identified. Ray tracing theory predictions may prove helpful in this endeavor, but the actual extraterrestrial particle shapes and compositions, perhaps affected by the presence of trace contaminants, could quite possibly be too complicated to model adequately.

Hence, in order to make better utilization of available space probe measurements, to assist in theoretical (i.e., ray tracing) methods for predicting extraterrestrial cloud scattering characteristics, and to aid in the determination of future *in situ* cloud measurement techniques, we proposed to conduct an experimental program of laser scattering and microphysical

measurements under controlled laboratory conditions. In order to simulate the clouds of the outer planets, a high vacuum, cryogenic chamber of sufficient volume to permit the growth of relatively large and complex crystals was clearly required. The clouds must then be produced under controlled conditions devoid of unwanted gaseous contaminants, and the means for directly observing and photographing the particles under a microscope must be provided for. Finally, the chamber must be constructed so as to permit the collection of laser scattering measurements from the clouds. Although backscattering measurements, for example, can be collected externally to the chamber through the use of a window through which to view the cloud, the determination of angular scattering phase function necessitates that either the laser source or the receiver unit be located and rotated within the chamber. In dealing with a cryogenic and sometimes caustic environment, the latter capability presents considerable technological difficulties which we were only partially successful in overcoming.

The design of our cloud chamber and laser scattering apparatus to fulfill the above requirements is described in detail in the next section.

2. The Experimental Design

2.1 The Planetary Atmosphere Simulation Chamber

Given in Fig. 1 is a scale drawing of the cloud chamber, and in Fig. 2 a schematic rendering of the plumbing associated with the vacuum, gas delivery and vent systems. The basic structures of these systems were constructed out of corrosion-resistant stainless steel and commercially-available high vacuum components whenever possible.

The cloud chamber has a total volume of 50 liters and is composed of an upper vertical "chimney" 92 cm by 21 cm diameter and a separable lower equipment bay 16 cm by 36 cm diameter. The two sections are bolted together and sealed with oversized fluorosilicone gaskets in an attempt to minimize the leakage experienced when standard Vitron vacuum gaskets were used earlier. Both parts are cooled by circulating liquid nitrogen (LN_2) under pressure through a pipe coiled about the cylinders. As shown by the cut-away view in Fig. 1, the entire chamber is encased in a 7.5 cm thick polyurethane foam insulating sleeve. Internal temperature is monitored at two locations within the chamber through the use of a flange-mounted dual thermocouple feed-thru. Chamber pressure measurement through a large dynamic range is accomplished with an atmospheric mercury manometer and thermocouple vacuum gage combination. Inserted through the top of the chamber is a sealed tube into which LN_2 could be poured to help glaciate supercooled liquid clouds by producing a localized chilling effect.

The chamber vent tube is provided with an atmosphere pressure check valve for safety purposes, but this device prevents the backflow of room air into the chamber as well. Potentially toxic or hazardous gases are exhausted from the chamber to a chemical hood vent by pressurizing the chamber with nitrogen

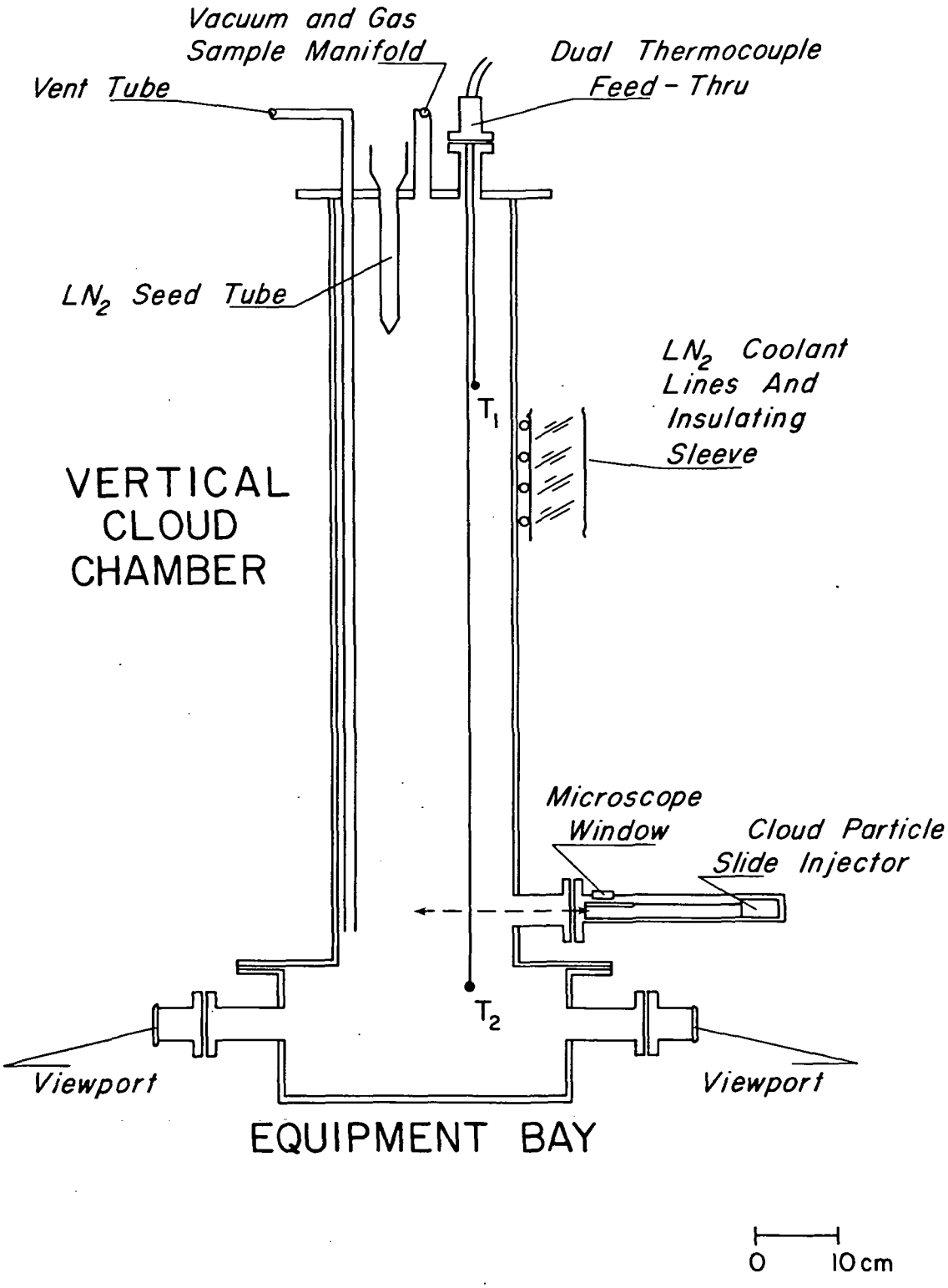

Figure 1 A scale drawing of the Planetary Cloud Simulation Chamber.

following an experiment. The gas supply manifold contains three separate lines with flowmeters so that mixed-gas atmospheres can be simulated (see Fig. 2). An additional line connects to a reservoir which can be filled with liquid samples (e.g., water) or, as was done in several experiments, with a powered substance which is mixed into an aerosol using compressed nitrogen and then allowed to enter the chamber to act as condensation or freezing nuclei. While cooling and evacuating the chamber a liquid nitrogen trap is used to remove volatile substances from the chamber and to prevent the back-flow of organic contaminants from the vacuum pump.

For cloud microphysical studies, sedimenting cloud particles are collected on a glass slide which is injected into the center of the lower chamber through a flange-mounted mechanism (see Fig. 1). The slide is then withdrawn and positioned under a gasket-sealed glass window through which microscopic observations and photomicrography are permitted. Originally, the slide was injected by magnetically coupling the holder to external sliding magnets. Although this method worked satisfactorily, it did not permit the installation of a temperature control system to cool the slide injector housing. Hence, to prevent the rapid melting or sublimination of the collected particles once positioned under the microscope, the original device was replaced by a linear motion feed-thru and plumbing for direct LN_2 cooling of the housing was installed. The current sampling device, however, requires careful temperature monitoring to prevent room air leakage through the vacuum gaskets which can become frozen. The microscope window is also bathed in dry nitrogen to prevent fogging. Illumination for the 35 mm camera photomicrography is provided through the microscope.

The lower equipment bay is fitted with two flange-mounted viewports for

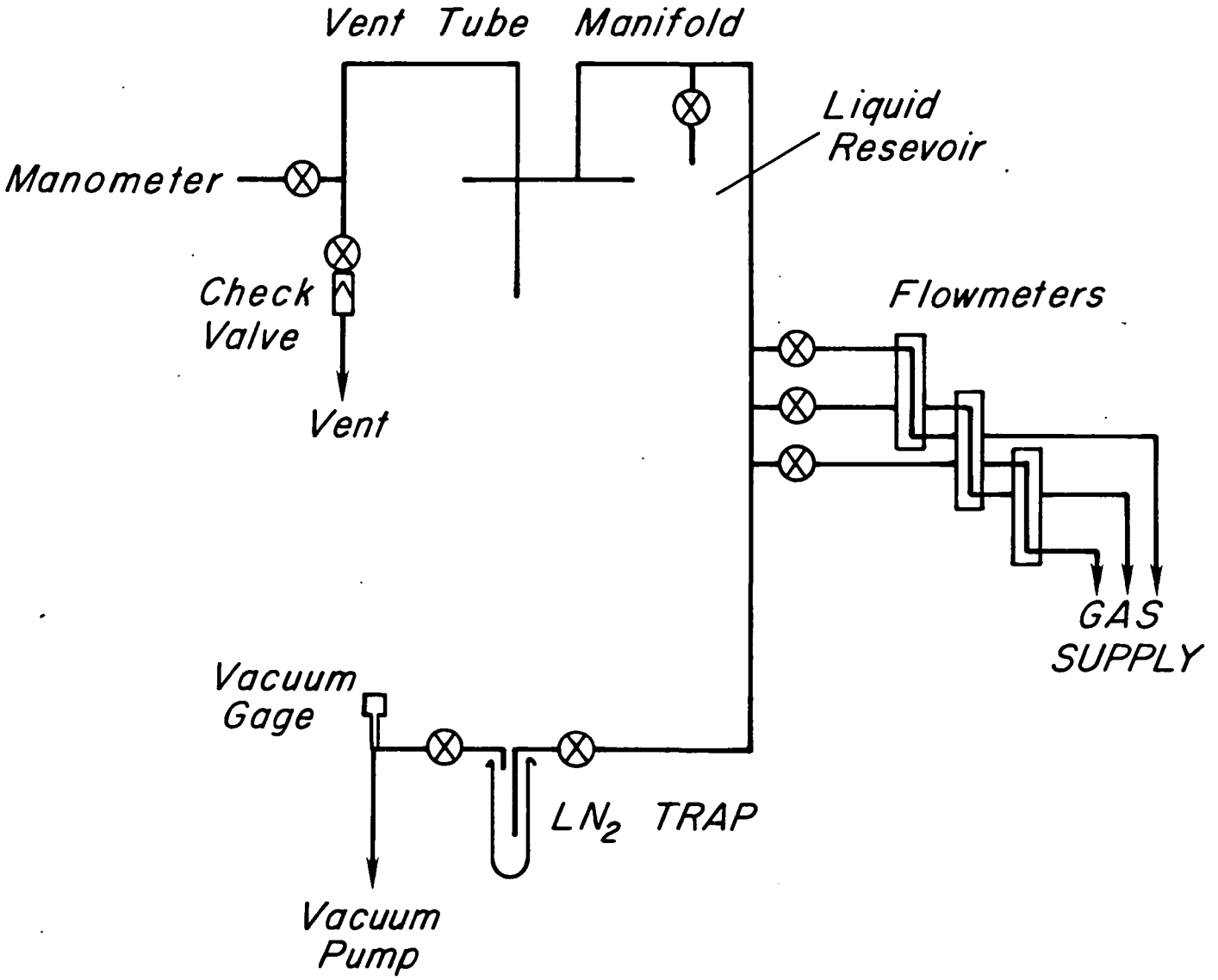

Figure 2 A schematic rendering of the plumbing associated with the Planetary Cloud Simulation Chamber. Circles with crosses represent high vacuum valves.

observing the cloud and for laser scattering studies. These glass-to-metal bonded, high vacuum windows are heated during experimentation with electrical heating tapes to prevent external fogging and internal cloud particle deposition.

2.2 Cloud Formation Techniques and Difficulties

Normally, after evacuation, the chamber is filled with one atmosphere of dry nitrogen gas and the cooling cycle is begun by circulating the LN_2. Since the chamber top, where the LN_2 is first introduced, cools rapidly, a large temperature gradient quickly develops due to the poor thermal characteristics of stainless steel and the rapid vaporization of the circulating LN_2. Hence, the most satisfactory way of producing a reasonably isothermal chamber environment is to cool the entire chamber down to near LN_2 temperatures and then allow it to warm slowly to the desired experimental temperature. The gas or gas mixture to be studied is then allowed to enter the chamber at a constant flow rate. Additional nitrogen gas may be used as a carrier gas, or the nitrogen originally present may be evacuated from the chamber prior to inserting a planetary gas mixture.

There are, however, two problems to be overcome in producing the clouds. The first is related to the formation at low temperatures of hazes which affect or even obscure the scattering properties of the desired clouds. In many cases, the hazes formed as a result of trace contaminants present in the gas supply cylinders. This source of contamination has been minimized by procuring the purest gas samples (electronic grade or better) possible. The other source of the haze results from room air leakage through frozen gaskets. The use of fluorosilicone gaskets at critical locations improves the integrity of the chamber, but it should be noted that even this substance

is not rated as effective at LN_2 temperatures. The flange and feed-thru gaskets within the slide sampling mechanism have been particularly sensitive to minor leakage problems, as this unit is directly cooled with LN_2, and several major leakage episodes have occurred during experiments. And, as discussed below, the rotary feed-thru assembly which we constructed for the angular scattering experiments was also prone to severe leakage.

The second problem area is in cloud formation itself. Particularly for pure carbon dioxide clouds, which lack a liquid phase at our chamber temperatures and pressures, cloud formation is difficult to initiate. The air within the chamber becomes quite devoid of particulates over successive experiments so that condensation or freezing nuclei are absent, resulting in the formation of only frost on the walls of the chamber. Attempts have been made to overcome this problem by introducing an aerosol (usually kaolinite) or a minute quantity of water vapor into the clouds.

2.3 The Backscattering Apparatus

Experiments were conducted using the basic lidar analog setup shown in Fig. 3 to obtain backscattering depolarization ratios from the simuluated clouds. Although most measurements were obtained using a continuous-wave 5 m W helium-neon laser at 633 nm, a series of measurements were also collected at 838 nm through the use of a continuous-wave 7 m W Gallium-Arsenide laser diode to gain experience for application to the angular scattering experiments.

For the visible laser light backscattering studies, the laser beam was aligned so as to pass through the centers of the two viewports. The laser was mounted on an optical rail on a table positioned 1.8 m from the cloud

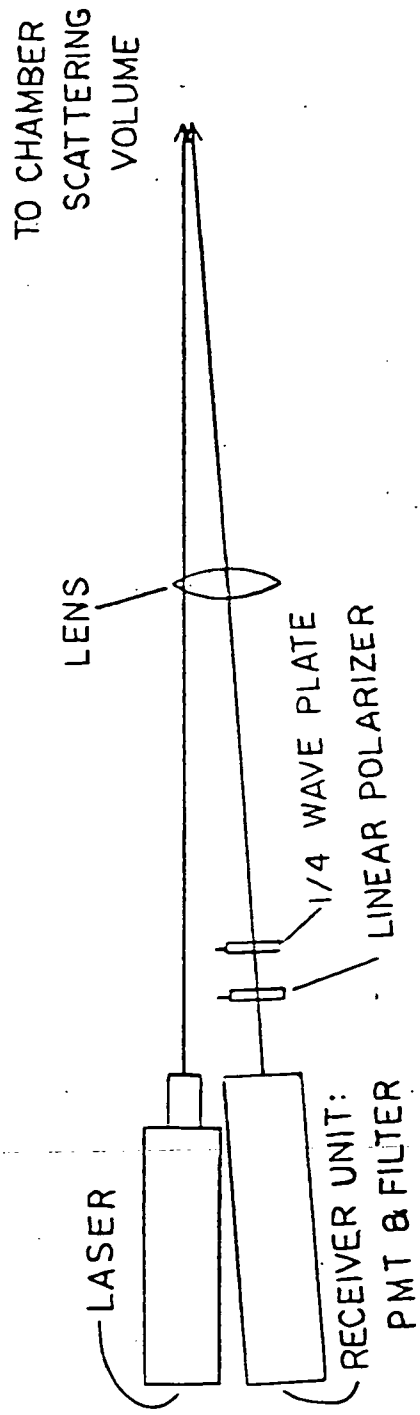

Figure 3 Lidar analog design for helium-neon laser backscattering studies, including complete Stokes parameterization.

chamber center. The laser emitted vertically-polarized radiation, and the polarization properties of the light backscattered from the cloud particles was determined with a receiver unit consisting of a 10 cm diameter lens, a polarization analyzer unit and a RCA 7265 photomultiplier tube (an extended 5-20 PMT) with an appropriate laser line filter. The analyzer components included a zero-order quartz 1/4 wave retardation plate and a high transmission polarizing filter mounted in rotatable supports, and a pinhole assembly to control the amount of light entering the PMT. The receiver unit was also mounted on an optical bench and was placed adjacent and at a slight angle to the laser bench (see Fig. 3). This arrangement allows for the measurement of scattered energy at as close to the backward direction as possible in the laboratory. The laser beam itself is passed through a small notch in the side of the receiver collecting lens, so that backscattering between the angles of 177.2 to 179.8° is analyzed. This particular design also allows the derivation of the complete Stokes parameters of the backscattered energy.

The configuration for the near-infrared studies differed in several respects. The compact laser source, a Laser Diode Model LCW-30 with internal collimation design (<5 mrad FWHM divergence), was adhered to a small section of acrylic linear polarizer and positioned directly against the forward viewport. The laser energy backscattered from the chamber passing around this device was collected by a receiver with a 10 cm lens, rotatable linear polarizer, and a RCA C31034 PMT contained within a dry ice cooled housing to suppress thermal noise at this wavelength.

In both cases, cloud extinction and optical thickness (see Section 2.4) were measured by monitoring the decrease in laser power due to the cloud as

the laser beam traversed the chamber. A Spectra-Physics Model 404 power meter, positioned ~1 m behind the far viewport, was aligned axially with the viewports and used for this purpose. The signals from the PMTs were first amplified with a Keithly Model 417 Picoammeter and then recorded on a multi-channel strip chart recorder along with cloud-attenuated laser power and the two chamber temperature traces. The polarizer filter orientations, photomicrograph frame numbers and physical cloud observations were notated directly on the strip chart record.

2.4 The Angular Scattering Apparatus

A number of different methods were explored to obtain the angular scattering phase functions. In general, it became apparent that the laser source should be mounted on a rotatable (through 2π) assembly within the lower bay of the chamber, permitting the observation through a viewport of scattered energy as a function of scattering angle from an external receiver, as previously described. Cloud attenuation could be monitored by placing a photodiode (mounted within a light trap of the glass horn design) on the rotating bench directly opposite the laser source. The receiver and photodiode signals could be stored, as a function of scattering angle, on a digital storage oscilloscope with a magnetic disk drive so that the raw data could be processed by a microcomputer after data transfer via an RS-232 interface.

With these scattering measurements, it is possible to derive normalized scattering phase functions from the data and interpret them in terms of the cloud microphysical data also concurrently collected. As a function of the scattering angle θ, the absolute power $P_s(\theta)$ is derived from the measured signal $I(\theta)$ and the receiver gain G_r,

$$P_s(\theta) = I(\theta)\, G_r \,. \tag{1}$$

This quantity can be related to the volume backscattering coefficient $\beta_s(\theta)$ $[m^{-1}\ sr^{-1}]$ of interest through the use of an analog of the lidar equation (adapted to continuous-wave laser operation), as follows

$$P_s(\theta) = \frac{P_i}{A_b} \frac{V(90°)}{\sin\theta}\, \omega_r\, \beta_s(\theta)\, \exp\,(-\sigma\, R)\,, \tag{2}$$

where P_i is the incident laser power measured prior to cloud formation, A_b the cross-sectional area of the laser beam in the scattering volume, $V(90°)$ the scattering volume at $\theta = 90°$, ω_r the solid angle of light scattered from a particle which is viewed by the receiver, and where the exponential term accounts for the attenuation of the laser beam after traversing the cloud. The first two terms define the laser power density and the change in the scattering volume with angle, respectively. The last term approximates the attenuation from Beer's law in which all scattering is removed from the propagating beam. The extinction coefficient σ $[m^{-1}]$ is defined in this case as

$$\sigma = -\frac{1}{R}\, \ell n\, \frac{P_r}{P_i}\,, \tag{3}$$

where R is the path length of the beam in the cloud and P_r is the laser power measurement after traversing the cloud.

Substitution of Eq. (3) into Eq. (2) and rearranging now yields the simplified expression for $\beta_s(\theta)$,

$$\beta_s(\theta) = \frac{P_s(\theta)\, A_b \sin\theta}{P_r\, \omega_r\, V(90°)}\,, \tag{4}$$

from which the normalized scattering phase function $P(\theta)$ can be obtained as shown below:

$$P(\theta) / 4\pi = \beta_s(\theta) / 2\pi \int_0^{2\pi} \beta_s(\theta) \sin\theta \, d\theta \quad . \qquad (5)$$

As the near-infrared spectral region is of particular interest to NASA investigators from both an active and passive remote sensing standpoint, and since laser diode devices are compact and relatively rugged, the components of the laser diode backscattering apparatus described in the last section were incorporated into these experiments. It was intended that the nephelometer rotation shaft, coupled to a stepping motor mounted below the center of the lower equipment bay, would contain an electrical feed-thru to power the laser emittor and photodiode. However, preliminary tests to determine the viability of standard laser diodes under the harsh environmental conditions within the chamber, using low-cost pulsed emittors, indicated an unacceptable frequency of failures due to the stresses of temperature recycling during repeated experiments. Moreover, a high power, cryogenic laser diode device which was designed to tolerate such conditions was dropped from production by Laser Diode Laboratories, and so could not be used as originally intended.

Hence, design changes were made to accomodate the use of a rotating fiber optics assembly so that the laser source could be coupled to the fiber optics bundle externally to the chamber. The preliminary design incorporated a commercially-available, high vacuum rotary feed-thru and a specially constructed fiber optics device. The fiber otpics bundle, 60 cm long and 0.3 cm diameter, was encased in a flexible, vacuum-tight stainless steel sleeve (0.8 cm diamter) and fitted with a special lens hood for final beam collimation.

Despite the laser power losses caused by this design change, signal-to-noise estimates indicated the likelihood of sufficient signal strengths with the available laser in the weak side-scattering region, at least for the known properties of water droplet clouds.

Unfortunately, the high-vacuum rotary feed-thru for which the fiber optics bundle was designed was dropped from production before it could be acquired. Within the budget and time restrictions remaining in this research project, it was attempted to convert a low-cost open tube feed-thru to one which would permit the rotation of the fiber optics/laser assembly. This device, however, clearly failed to maintain the vacuum integrity of the chamber when the assembly was rotated, and could not be applied to angular scattering studies.

3. The Experimental Results

3.1 Selection of the Simulated Atmospheres

The abundances of planetary gases in the region of the solar system extending from the planets Mars to Saturn, the focus of this investigation, are reasonably well known. The primary cloud forming materials are likely to be water ice, solid carbon dioxide, and solid and liquid ammonia and methane. The chemical composition of the thin Martian atmosphere is dominated by CO_2, with perhaps significant amounts of A_r and N_2, and trace but variable quantities of H_2O, CO, O_2 and O_3 (see, e.g., Moroz, 1976). As for the Jovian and Saturnian atmospheres, H_2 is dominant, followed by H_3 and a number of trace constituents including CH_4, NH_3, H_2O and other ogranic and noble gases (e.g., Ingersoll, 1976; Treffers et al., 1978; Ingersoll et al., 1980). It appears that upper atmospheric temperatures are cold enough to support methane clouds only on the planet Saturn from this group.

The exact compositions of the clouds are still the subject of considerable speculation. Only Mars has a simple enough atmosphere to point convincingly to the presence of water ice and perhaps mixed CO_2 and H_2O clouds. In the Jovian atmospheres, complex organic substances may be important cloud forming materials, perhaps explaining the wide variety of cloud colors observed, but ammonia in the liquid and solid phase, and mixed with water, are commonly mentioned as major cloud constituents, along with ammonium hydrogensulfide, NH_4SH (Newburn and Gulkis, 1973; Ingersoll, 1976; Rossow, 1978). Given in Table 1 are the gas mixtures selected for microphysical and scattering studies. Although these ten atmospheric compositions by no means exhaust the possible cloud forming combinations, they do represent a reasonable starting point to better understand the cloud formation and optical

Table 1. Summary of simulated atmospheric compositions.

Principal Gases	H_2O	CO_2	NH_3	CH_4
	N_2	N_2	N_2	N_2
Admixed Gases	Atmos-pheric*	He	CH_4	He
		H_2O*	H_2O	

*Studies using both 633 and 838 nm laser wavelengths.

properties of the planetary atmospheres of the outer planets. Compiled in Table 2 are some known physical properties of the four, pure cloud forming materials.

Table 2. Some physical properties of the cloud forming substances tested, compiled from various sources.

Substance	Boiling point at 1 atm	Melting point at 1 atm	Real Index of Refraction	
			liquid	solid
Water (H_2O)	373°K	273°K	1.333	1.3
Ammonia (NH_3)	240°K	195°K	1.355±0.005	1.415±0.005
Carbon Dioxide (CO_2)	not applicable	194.5°K (sublimation point)	not applicable	not found
Methane (CH_4)	114°K	90.4°K	1.30±0.01	1.33±0.01

3.2 Backscattering Linear Depolarization and Microphysical Measurements

3.2.1 Pure Liquid Phase Clouds

It is a fundamental principle that homogeneous spherical scatterers should produce no depolarization of the incident electromagnetic wave during single backscattering. Hence, liquid phase particles of any composition whose surface tension force dominates over aerodynamical stresses should produce zero depolarization. That this is not the case when terrestrial water clouds are probed with lidar is known to be due to the result of the finite receiver viewing multiple scattered photons (see, e.g., Pal and Carswell, 1973). It has been established through theoretical simulations that the amount of depolarization measured from water clouds is primarily a function of lidar beamwidth design and cloud optical thickness, with droplet size distributions also having an effect on the multiple scattering process (Liou and Schotland, 1971).

In the laboratory environment, the amount of multiple scattering-induced depolarization measured can be expected to be related to the extinction coefficient σ of the cloud (Sassen and Liou, 1979). Figure 4 illustrates this phenomenon for typical pure liquid phase clouds composed of water, ammonia, and methane for temperatures above their respective melting points. The linear depolarization ratio δ is defined as

$$\delta = E_{\perp} / E_{\parallel} \quad , \tag{6}$$

where $E_{\perp}$ and $E_{\parallel}$ are the returned laser energies in the planes of polarization orthogonal and parallel to the plane of the vertically polarized laser sources used in this investigation. Both the liquid water and ammonia clouds show a δ versus σ relationship which is quite similar to that found previously

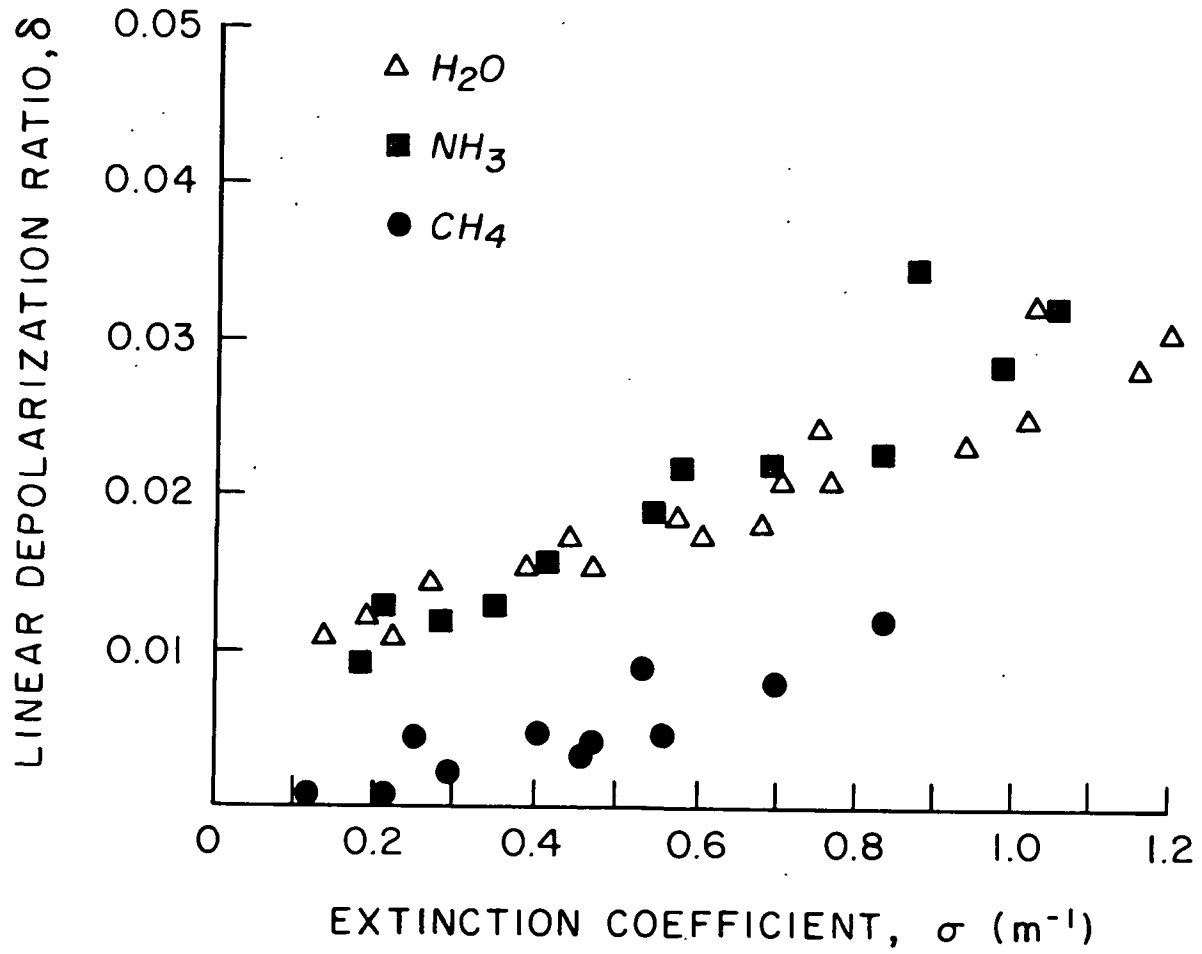

Figure 4 The dependence of linear depolarization ratios on extinction coefficient for three types of liquid clouds. The laser depolarization from these clouds results from multiple scattering activity, and appears to increase linearly with optical depth.

for vertically polarized laser light in water clouds (Sassen and Liou, 1979). The results for the methane clouds, however, indicate significantly lower depolarization values from multiple scattering activity. This finding may be attributable to strong laser wavelength (633 nm) absorption due to liquid and/or gaseous methane, or may perhaps be a result of differences in the droplet size distributions typical of our simulated clouds.

3.2.2 Pure Solid Phase Clouds

Through recent developments in ray tracing simulations of the scattering behavior of nonspherical particles larger than the incident wavelength, the experimental findings suggesting that the backscatter depolarization technique should be quite sensitive to particle shape are being confirmed. The amount of depolarization measured in the backscatter from crystalline particles depends on the index of refraction of the solid substance and the exact internal and external scattering geometry for each particle symmetry integrated over all possible crystal orientations. Hence, various cloud particles with different characteristic shapes should produce backscatter linear depolarization ratio "signatures". The degree to which our experimental findings support this basic premise is shown in Fig. 5.

In Figure 5, the δ values for pure solid clouds of the four cloud forming substances are shown as a function of temperature. In general, the δ values for each cloud type are distinct. The scattering and microphysical properties of these pure clouds are discussed separately below. Note that highly purified nitrogen, and occasionally helium gas were used as carrier gases during the experiments (see Table 1). These gases are presumed to be non-interactive with the cloud forming gases, and no noticeable differences were found when

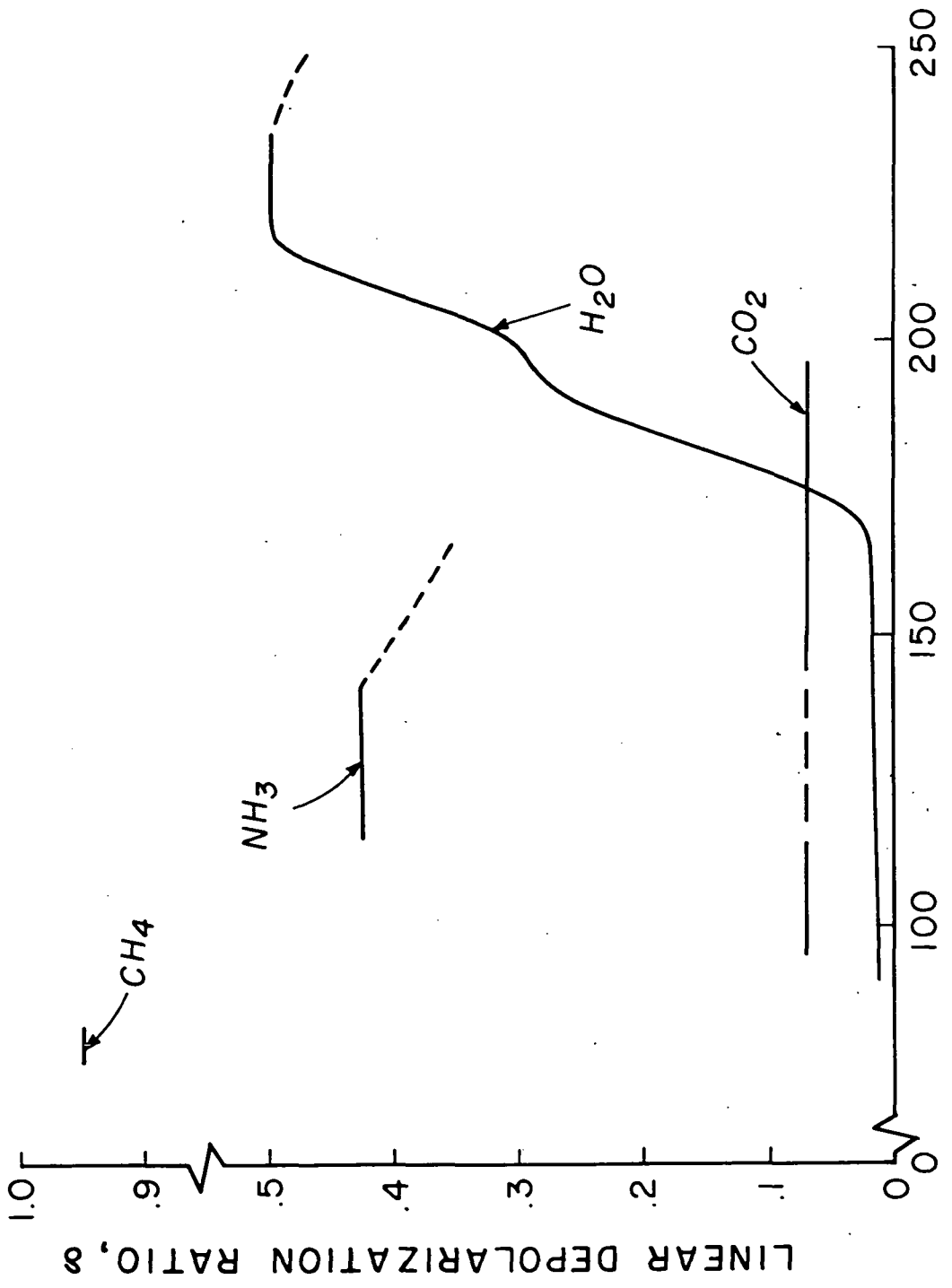

Figure 5 The dependence of backscatter linear depolarization ratios on chamber temperature for the indicated solid phase clouds. Short dashed lines indicate a mixed solid and liquid phase composition.

N_2 or H_e were used.

Water Ice Clouds. Water ice clouds grown in pure nitrogen and through the use of atmospheric (room) air yielded quite similar δ values which were a strong function of temperature. No significant differences were noted in the δ values at either the 633 or 838 nm wavelengths. The striking behavior of the δ value decreasing trend with decreasing temperature shown in Fig. 5 appears to be related to known changes in ice particle shape (see Hobbs, 1974), and is supported by our available microphysical observations.

At the temperatures normally encountered in the earth's troposphere, ice forms hexagonal crystals with δ values ranging between 0.4-0.5 for pristine ice clouds and precipitation particles. Pure liquid water, however, can be supercooled to ≈40°K below the melting point, and sub-freezing clouds are often noted to be of mixed-phase composition. Our data show the $\delta \approx 0.5$ value characteristic of pure ice clouds between the temperatures of 215-235°K, with, on the average, decreasing δ values for $\gtrsim$235°K reflecting the presence of mixed-phase clouds. At temperatures between 85-175°K, water ice δ values are on the order of a few percent, and display multiple scattering-induced δ increases at high optical depths. This behavior is consistent with spherical or near-spherical vitreous ice particles in agreement with expectations (Hobbs, 1974). Microscopic observations of the chamber particles within this temperature range reveal the presence of minute (<10 μm) amorphous particles which, although difficult to resolve clearly, lack the reflecting surfaces of ice crystals.

The cause of the gradually changing depolarizing behavior of ice clouds between 175-215°K appears to be a consequence of mixed particle types, in which the vitreous ice mode becomes increasingly dominant with decreasing

temperature. However, the presence of cubic ice crystals is often cited for temperatures ≤200°K, and the discontinuity at this temperature in the δ value curve of Fig. 5 may be attributable to the appearance of these crystal shapes. It is interesting to note that the same depolarizing behavior is noted by either slowly warming an ice cloud or by creating successive ice clouds within the chamber at various temperatures. Although the "ledge" in the δ value curve is sometimes less pronounced when the former method is used, it follows that the ice particles can readily transpose from one structure to another with changing temperature, as expected from earlier studies (see Hobbs, 1974).

Unfortunately, it has been found quite difficult to resolve the shapes of ice particles collected from our chamber at these temperatures due to their small size, microscopic observing power limitations, and their tendency to evaporate quickly under illumination. Figure 6 is a photomicrograph of water ice particles collected at a temperature of 190°K and a pressure of 350 mb, using a water vapor augmented atmospheric air sample. Each grid box in this and the following photomicrographs is 135 μm on a side, and the difficulties inherent in resolving the particle shapes are apparent. Nonetheless, there is often visual evidence for hexagonal and cubic reflecting surfaces, and for spherical particles displaying a bright central dot under microscopic illumination.

Carbon Dioxide Clouds. Although, as previously mentioned, CO_2 ice clouds were typically quite difficult to nucleate, once generated as a result of the introduction of artificial nuclei (aerosols or water ice germs), these clouds were comprised of relatively large and complex crystals (Sassen, 1981). Despite the strong backscattering and complex crystal shapes, however, δ values

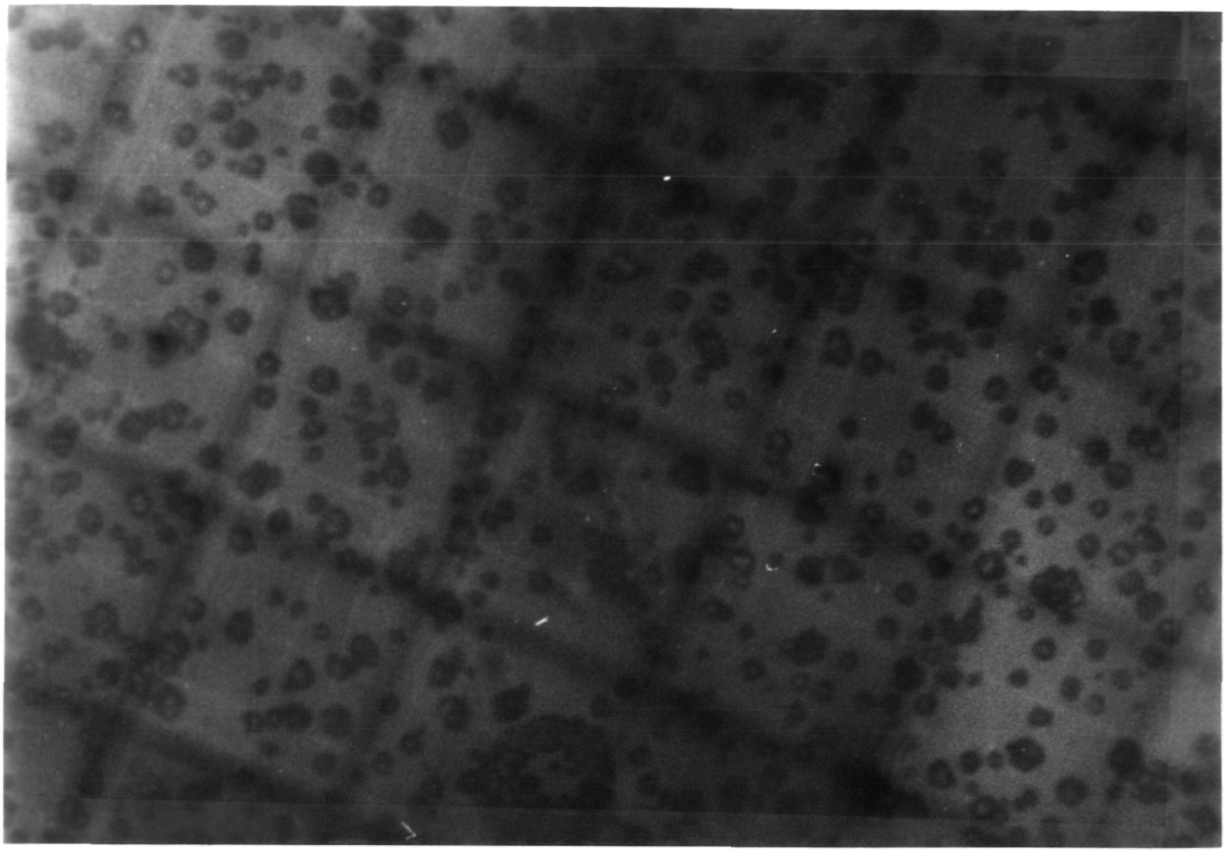

Figure 6 Minute water ice particles grown within the chamber at a temperature of 190°K. Each grid box is 135 μm wide.

remained at ~0.07 through the temperature range of 95-195°K (see Fig. 5). Such low depolarizations may be due to strong laser (633 nm) light absorption within the crystals, but the index of refraction of solid CO_2, either real or imaginary, could not be found after an extensive search of the literature to prove or disprove this possibility. Although hazes from gas sample contaimination were often present (particularly between 120-140°K), we feel it is unlikely that they significantly affected the δ values from dense CO_2 clouds.

To illustrate the particle types produced during the experiments, Figures 7 and 8 are given. Despite the significant difference in temperature, pressure, amount of N_2 carrier gas, and nucleation method (see figure captions), the crystal shapes appear to be similar. The crystals often appear to have hexagonal cross sections with triagonal, and occasionally square reflecting surfaces. Although many crystals have quite complex shapes and display internal structures, others resemble solid single or doubled hexagonal pyramids.

Ammonia Ice Clouds. Analogous to the situation for water ice clouds, liquid ammonia droplets were capable of surviving considerable supercooling before freezing into crystals. With reference to Table 2, since pure ammonia ice clouds are believed to have occurred only $\lesssim$145°K, some 50°K of supercooling below the melting point was observed during most of our experiments. As shown in Figure 5, solid ammonia clouds produced average δ values of 0.42

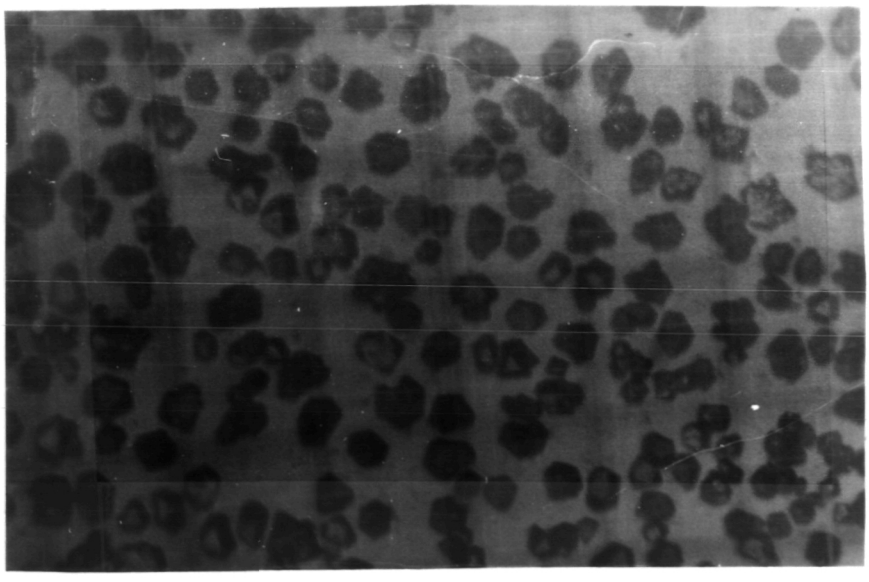

Figure 7 Carbon dioxide crystals produced at 105°K at 8 mb pressure primarily of CO_2 gas. The crystals were nucleated on kaolinite particles injected into the chamber with pulses of N_2.

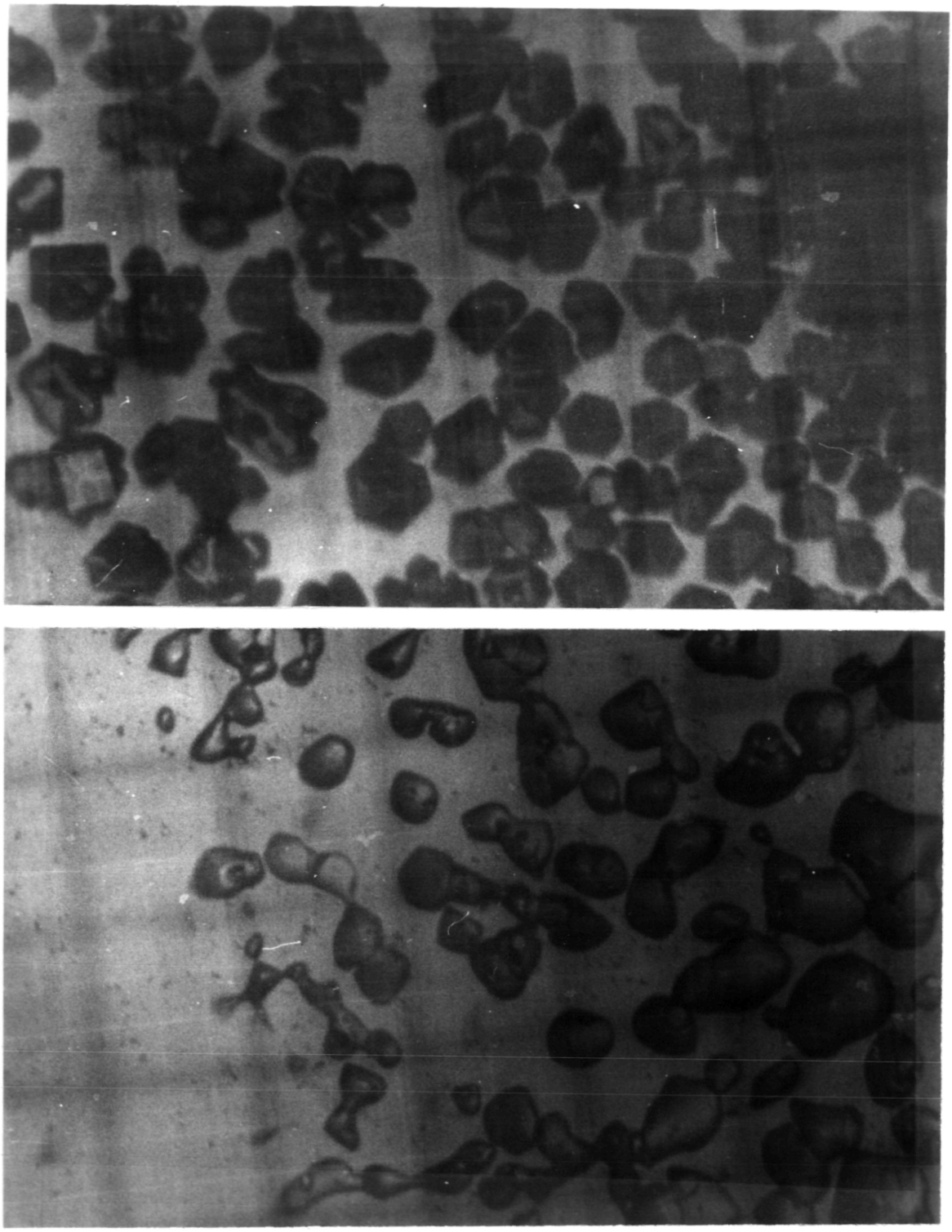

Figure 8a-b Carbon dioxide crystals nucleated at 145°K and 840 mb pressure, primarily of N_2, through the introduction of a pulse of impure N_2 gas. As shown in b (bottom), the rapid sublimation of the particles under microscopic illumination produced rounded crystal forms but no noticeable solid or liquid residue.

between 115-143°K, varying between 0.36-0.45 perhaps as a consequence of contamination from hazes. The dashed line in the figure illustrates the typical depolarizing behavior noted as ammonia ice clouds were gradually warmed -- the decreasing δ values are believed to represent the appearance of supercooled liquid drops as the existing ice particles sedimented to the bottom of the chamber. However, it should also be mentioned that a few experiments using another, but similar grade NH_3 gas sample at temperatures between 96-110°K produced thick clouds of primarily liquid droplets which displayed low δ values (0.02-0.05). Whether these particles represent some form of contaminant haze, extremely supercooled ammonia (~100°K) droplets, or an ammonia/contaminant mixture is uncertain, but typical ammonia crystals were nucleated from these clouds when LN_2 was poured into the seeding tube at the top of the chamber. The δ values produced ranged from 0.18-0.25, perhaps reflecting a mixed-phase cloud environment. Due to the possibility of gas sample contamination, these data are omitted from Fig. 5.

It is usually difficult to clearly resolve ammonia ice crystal shapes from the photomicrographs, such as Figure 9, because of the rapid rate at which the particles melted under powerful microscopic illumination. Visual inspection at lower light levels of the particles collected on the slide were more useful for identifying the crystal habits. Ammonia crystals, grown in ~200 mb of N_2, for example, were found to be large (~70 μm) pyramidal crystals at 96°K, and at 110°K high concentrations of smaller crystals displaying both square and triagonal reflecting surfaces were observed. We conclude that pure ammonia ice crystals are most likely to assume a cubic structure involving five-sided pyramids and perhaps cubic crystals as well. This is at variance with the recent findings of Tomasko (personal communication)

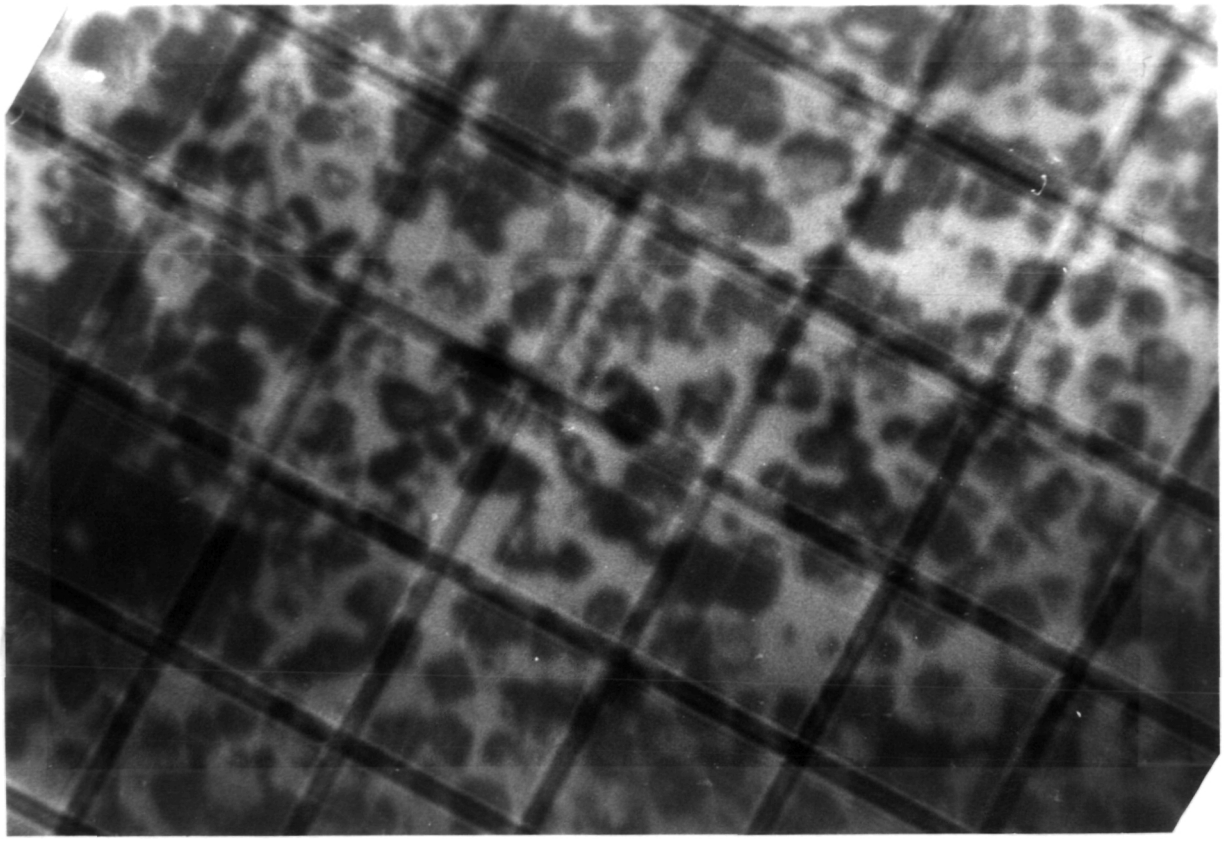

Figure 9 Photomicrograph of ammonia crystals which have begun to melt, grown at 115°K and at 320 mb of primarily nitrogen. Several crystals with square cross sections can be identified, indicating cubic or five-sided pyramidal crystals.

who has observed four-sided pyramids.

Methane Ice Clouds. Although liquid methane clouds are easily produced at temperatures >110°K, we have been successful in producing methane ice clouds on only a few occasions through the use of the LN_2 seeding tube. In all cases, dense clouds of particles were formed which rapidly fell out and dissipated. These clouds were produced at the minimum internal chamber temperature of ~90°K, with total pressures (approximately equal amounts of CH_4 and N_2 or He) of 50-100 mb. As seen in Fig. 5, the δ values from these short-lived

solid phase clouds averaged 0.94. Such high depolarizations are unique in our experience, and suggest very complex crystal shapes (perhaps dense radiating dendritic growths of multi-faceted crystal elements). Unfortunately, the temperatures at which these particles were produced prohibited microscopic examination with the cloud sampling technique used.

3.2.3 Cloud Mixtures

A number of atmospheric constituents display overlapping ranges of boiling and melting point temperatures, and so it is possible that these substances may combine to produce cloud particles of new types in some regions of planetary atmospheres, if the gaseous abundances are appropriate. Hybrid particle types may also result from the incorporation of trace gases into the crystal lattice of growing particles. Realistically, the possibility that the experimental results for the "pure" clouds described above may have been affected in some way by the trace contaminants in the gas samples used cannot be discarded. Nonetheless, we identified three gaseous mixtures (accompanied by N_2) which would be likely candidates for producing mixed-substance cloud particles, as described below.

Carbon Dioxide and Water Ice. In view of the difficulty in generating solid CO_2 clouds, trace amounts of water vapor were used to provide nuclei for particle growth with apparently no effect on CO_2 particle characteristics. However, when a CO_2 atmosphere was mixed with more significant amounts of water vapor (in nitrogen gas) supplied from a heated vessel containing distilled water, new types of particles were produced which resembled neither crystal habit in the pure phases at the chamber temperatures. Shown in Figure 10 is a large (~0.6 mm long) frost crystal found under these conditions

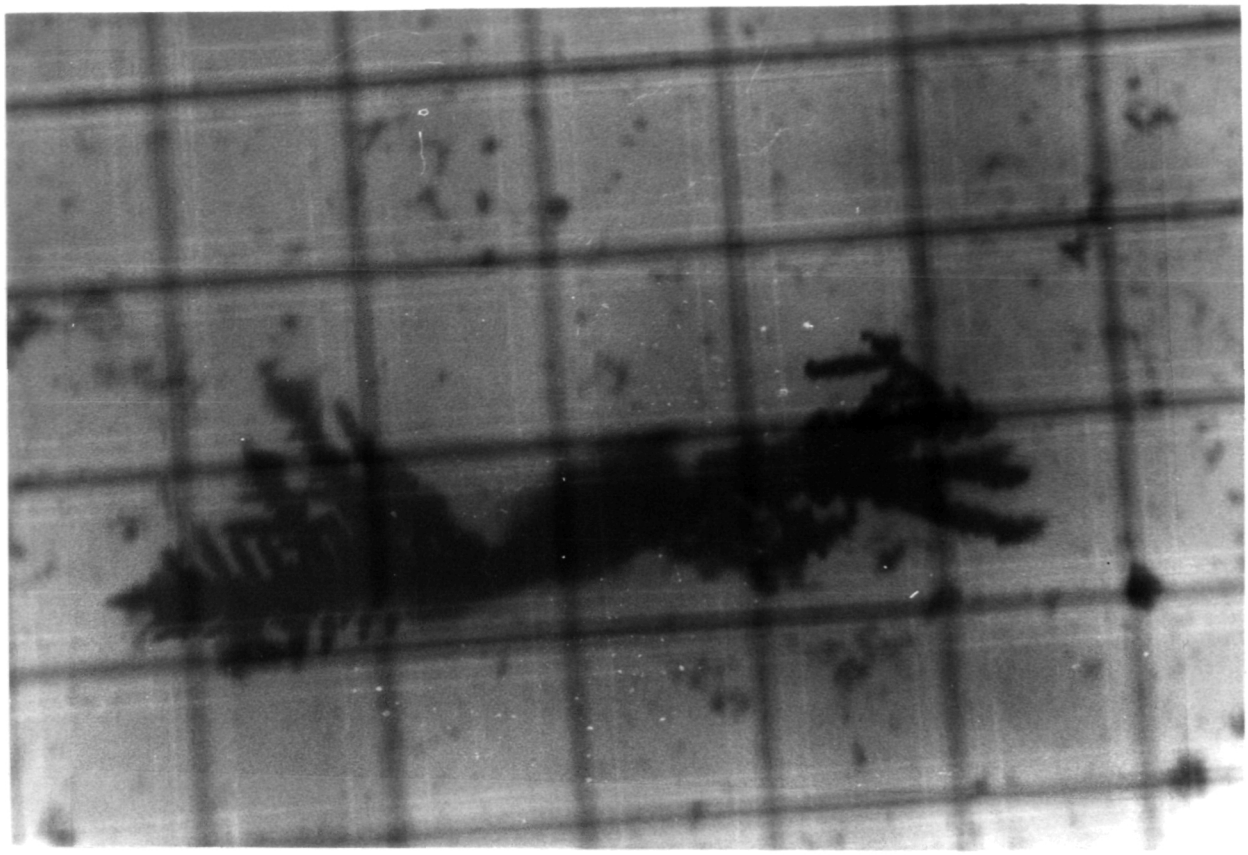

Figure 10 A large frost crystal grown in a mixed CO_2, H_2O and N_2 environment displaying a dendritic structure. This particle formed at a temperature of 180°K and total pressure of 585 mb.

which was captured following an experiment after falling from the chamber wall. Most of the cloud particles themselves resembled masses of amorphous particles, many of which displayed radiating branches. That a combined CO_2/H_2O growth mode occurred is supported by the observation that, as the crystal branch heated up under microscopic illumination, the structure first began breaking apart (due to CO_2 sublimation) before the remainder melted. Values of δ for these mixed clouds varied between 0.2-0.3 for temperatures between 160-200°K, which, although close to those for pure ice at the warmer temperatures, are considerably larger than the δ values for the single particles

of the vitreous phase of ice produced in the chamber in a pure H_2O/N_2 environment.

It is interesting to note that the dendritic branches of the frost crystal shown in Fig. 10 are positioned at an angle of ~60° from the main crystal branch, and therefore closely resemble a dendritic crystal of pure ice. The evidence suggests then that, at least for the atmospheric mixtures tested in these studies, the mixed particle structure was dominated by the growth of water ice. Komabayasi (1970) has reported similar dendritic structures for pure CO_2 clouds, but it now appears that contamination from water vapor may be responsible for his findings.

Ammonia and Water Vapor. We have found strong evidence that the combined growth of these two substances can lead to new ice particle types and also lead to the formation of complex aerosols following cloud droplet evaporation in planetary atmospheres. Water vapor introduced into liquid ammonia clouds did not produce any ice crystal fallout, indicating an absorption of the water vapor by the ammonia droplets. However, the subsequent warming or cooling of the chamber produced different results. After allowing the liquid cloud to evaporate, minute aerosols comprised of radiating needle crystals of ammonium salts were collected. Glaciating the droplet clouds through the use of the LN_2 seeding tube generated high concentrations of minute multi-faceted crystals. As the particles collected on the slide melted and evaporated, large assemblies of radiating salt crystals were observed to grow from the residue (Figure 11). Although it is possible that water vapor was adsorbed by the liquid ammonia during the rapid ice melting phase, the evidence suggests that the original crystals were comprised of ammonia hydrates derived from the frozen droplets. No scattering data are

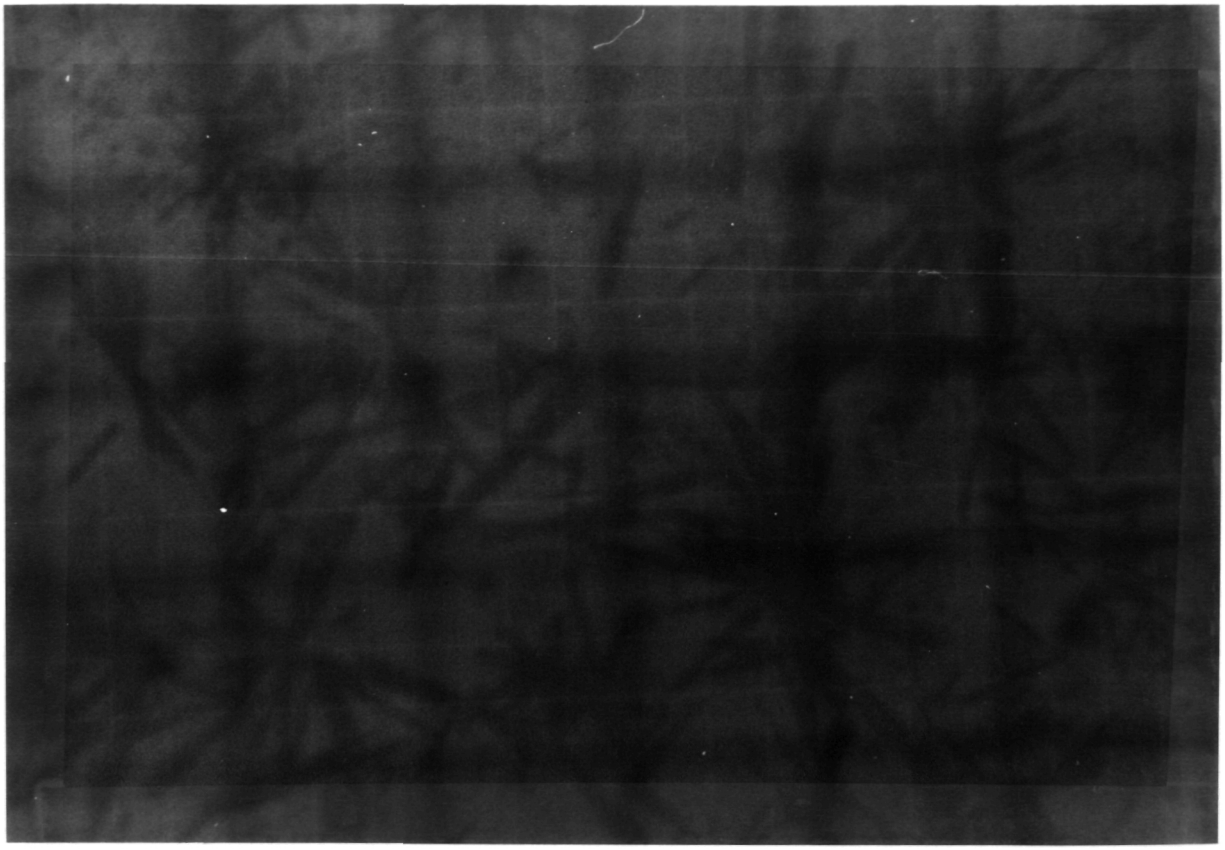

Figure 11 A residue of ammonium salt crystals left on the slide following the melting and evaporation of crystals grown at 127°K and 385 mb from a mixed ammonia, water vapor, and nitrogen atmosphere.

available for these microphysical experiments, however.

Ammonia and Methane Clouds. Similar experiments peformed using a mixed NH_3, CH_4 and N_2 atmosphere failed to indicate any changes in ammonia ice microphysical or scattering properties. The two substances appeared to form clouds independently of one another in one experiment performed at 105°K, in which δ values of ~0.25 indicated a mixed ammonia ice and liquid methane cloud. No solid methane clouds could be produced during these experiments.

3.3 Stokes Parameter Measurements

Complete Stokes parameterization of the backscatter was obtained in several experiments conducted with liquid and solid water, liquid ammonia, and carbon dioxide clouds. These data have provided fundamental knowledge of the nature of the backscatter depolarization process in both liquid and solid clouds, as has subsequently been verified under more controllable cloud conditions in our atmospheric cloud chamber (Griffin, 1983). The measurements reveal that, for either liquid or solid phase clouds, there is no statistically significant ellipticity or polarization plane rotation angle. The depolarization amounts expressed by the δ value can be almost entirely accounted for by the degree of linear polarization parameter P determined from the complete Stokes measurements. In other words, the change in the polarization properties of backscattered laser light is due to randomly polarized light from internal scatterings within nonspherical particles or from multiple scattering activity among spheres. This component is superimposed on the single scattering contribution from spheres, or the specular surface reflections from the crystalline faces on ice particles, which strongly preserve the incident polarization state. The depolarized component does not fit the true quantum mechanical description of randomly polarized energy, but rather is comprised of a collection of rays from many particles displaying a multitude of polarization ellipses which, at any instant, combine to produce backscattering lacking recognizable polarization ellipse properties. This is a consequence of high order multiple scattering and the almost infinite number of internal scattering ray paths possible from randomly oriented crystals of differing sizes and aspect ratios.

4. Conclusions

This laboratory research program has attempted to obtain a preliminary understanding of the microphysical and light scattering properties of planetary atmospheres whose true compositions and cloud forming processes are still only in the realm of speculation. The cloud forming processes and the substances themselves are certain to be exotic in comparison to terrestrial clouds. In attempting to simulate even simple extraterrestrial clouds, considerable technological problems have to be overcome. Moreover, for cryogenic applications, the purity of even the highest grade of commonly available gas sample cylinders is likely to be the source of some level of condensed or adsorbed contaminants. Nonetheless, we believe that our Planetary Simulation Chamber is a unique facility for extraterrestrial cloud studies, and with the exception of the unsuitability of the additional components required to obtain angular scattering measurements, this facility has performed well and most of our original experimental objectives have been accomplished.

A major goal of our program has been to investigate the suitability of the backscatter linear depolarization technique for discriminating the cloud forming substances found in the outer planets. With reference to Fig. 5 and the discussion in Section 3, it has been demonstrated that there is considerable potential for such an instrument to be used for planetary exploration, provided, of course, that our simulated clouds are representative of actual conditions. In considering these findings, several questions arise. Although the scattering behavior of water ice clouds seems to agree with our knowledge of the dependence of ice particle shape on temperature, the reasons for the relatively low depolarization values from

carbon dioxide clouds comprised of complex crystals, the uniquely high δ values for solid methane clouds, and the dissimilar multiple scattering characteristics of liquid methane clouds can only be speculated. Better knowledge of the optical constants of these substances are of fundamental importance to help answer these questions.

A significant development in our understanding of the scattering process by which laser light is depolarized during single and multiple scattering has followed from the measurements of the complete Stokes parameters in the backscatter. We have demonstrated that the light backscattered from dense assemblies of spheres or clouds of randomly oriented crystals larger than the incident wavelength is comprised of a combination of energy retaining the incident polarized state and a component which appears to be randomly polarized. A physical model to account for this finding has been developed.

Perhaps the most interesting findings that have come from this research have resulted from the cloud microphysical observations, and it is hoped that this knowledge will aid those investigators involved in extraterrestrial cloud diagnosis and modelling. The implications of our findings with regard to the cloud forming processes on Mars and the Jovian planets are summarized below.

Mars. Due to the absence on Mars of a liquid phase for carbon dioxide or water, it is perhaps only under unusual conditions that cloud formation can occur, although surface deposition in the form of frost is of course another matter. In our experiments, CO_2 crystals could only be generated after first introducing nuclei composed of mineral aerosols or water ice germs. The energy barrier for homogeneous deposition of gaseous CO_2 into

ice is certainly, as it is for water vapor (see Pruppacher and Klett, 1980), an enormous physical barrier. Hence, if water vapor in sufficient quantities is absent, then the transport of suitable surface-derived materials to the tropopause or other cloud-forming region must be considered. If sufficient water vapor is locally present, combined CO_2/H_2O particle growth may occur, or pure water ice in the vitreous or possibly cubic mode may form. In all cases, knowledge of the nature, transport, and abundance of ice forming nuclei is critical to the understanding of cloud formation in the thin Martian atmosphere.

Jovian Planets. Considerable speculation has occurred concerning the possible presence of Jovian clouds comprised of combined or separate water and ammonia particles. It should first be noted that in our experiments liquid ammonia droplets appear to display the ability to exist in a highly supercooled state, by as much as 50°K, or perhaps even 100°K. Hence, the presence of cloud temperatures below, even significantly, the melting point of ammonia should not automatically be assumed to be favorable for the formation of solid ammonia clouds. Many Jovian cloud models (e.g., Rossow, 1978; Ingersoll, 1976) place an outer ammonia ice cloud at the 140°K (700 mb) level, the approximate temperature at which our clouds began transforming into mixed solid and liquid phase particles.

The quantities and vertical distribution of water vapor relative to ammonia are likely to have a significant effect on Jovian cloud formation. Mixed ammonia-water solution clouds have frequently been postulated below the ammonia ice cloud, and such droplets may freeze to form ammonia hydrate crystals or evaporate to produce hazes of aerosols of ammonium salts in undersaturated regions. Whether a relatively pure water cloud could exist

at still lower levels under these conditions is uncertain. The picture is of course further complicated by the possible presence of other trace gases, such as H_2S, which would produce a more complicated cloud droplet and aerosol chemistry.

The cloud forming materials on Saturn are likely to be similar to those just discussed. Due to colder atmospheric temperatures of Saturn and the planets beyond, however, liquid methane, again likely significantly supercooled, may be an important cloud forming substance. At still colder temperatures, solid methane, and clouds of liquid nitrogen and the noble gases may be encountered. These additional inert cloud forming materials will be likely to form pure cloud particles and display significant supercooling before homogeneous (ice) nucleation occurs. However, if solid and supercooled liquid particles occur together, combined substance growth can occur through a scavenging process in which the solid particles collect the droplets of another substance, certainly a unique particle growth mechanism.

5. References

Cai, Q. and K.N. Liou, 1982: Polarized light scattering by hexagonal ice crystals: Theory. Appl. Opt., 21, 3569-3580.

Griffin, M.K., 1983: Complete Stokes parameterization of laser backscattering from artificial clouds. M.S. Thesis, University of Utah, 93 pp.

Hansen, J.E. and J.W. Hovenier, 1974: Interpretation of the polarization of Venus. J. Atmos. Sci., 31, 1137-1160.

Hobbs, P.V., 1974: Ice Physics. Clarendon Press, Oxford, 803 pp.

Ingersoll, A.P., 1976: The atmosphere of Jupiter. Space Science Reviews, 18, 603-639.

Ingersoll, A.P., G.S. Orton, G. Münch, G. Neugebauer and S.C. Chase, 1980: Pioneer Saturn infrared radiometer: Preliminary results. Science, 207, 439-443.

Komabayasi, M., 1970: Shape instability of crystals of ice, carbon dioxide and ammonia in a cold chamber. J. Meteor. Soc. Japan, 48, 270-286.

Liou, K.N. and R.M. Schotland, 1971: Multiple backscattering and depolarization from water clouds for a pulsed lidar system. J. Atmos. Sci., 28, 772-784.

Moroz, V.I., 1976: The atmosphere of Mars. Space Science Reviews, 19, 763-843.

Newburn, R.L. and S. Gulkis, 1973: A survey of the outer planets Jupiter, Saturn, Uranus, Neptune, Pluto and their satellites. Space Science Reviews, 3, 179-271.

Pal, S.R. and A.I. Carswell, 1973: Polarization properties of lidar backscattering from clouds. Appl. Opt., 12, 1530-1535.

Pruppacher, H.R. and J.D. Klett, 1980: Microphysics of Clouds and Precipitation. D. Reidel, Boston, 714 pp.

Rossow, W.B., 1978: Cloud microphysics: Analysis of the clouds of Earth, Venus, Mars, and Jupiter. Icarus, 36, 1-50.

Sassen, K., 1978: Air-truth lidar polarization studies of orographic clouds. J. Appl. Meteor., 17, 73-91.

_____, 1981: Laboratory study of Martian cloud microphysics. Third International Colloquium on Mars, Pasadena, Preprints, 219.

_____ and K.N. Liou, 1979: Scattering of polarization laser light by water droplet, mixed-phase and ice crystal clouds. Part I: Angular scattering patterns. Part II: Angular depolarization and multiple-scattering behavior. J. Atmos. Sci., 36, 838-861.

Treffers, R.R., H.P. Larson, U. Fink and T.N. Gautier, 1978: Upper limits to trace constituents in Jupiter's atmosphere from an analysis of its 5-μm spectrum. Icarus, 34, 331-343.

Whalley, E. and G.E. McLaurin, 1984: Refraction halos in the solar system. I. Halos from cubic crystals that may occur in atmospheres in the solar system. J. Opt. Soc. Amer., A1, 1166-1170.